

Learning-Assisted Multi-Operator Variable Neighborhood Search for Urban Cable Routing

Wei Liu^a, Tao Zhang^a, Chenhui Lin^b, Kaiwen Li^a and Rui Wang^{a,*}

^aNational University of Defense Technology, 109 Deya Road, Kaifu District, Changsha, 410073, Hunan Province, China

^bDepartment of Electrical Engineering, Tsinghua University, 30 Shuangqing Road, Beijing, 100084, Beijing Municipality, China

ARTICLE INFO

Keywords:

Distribution network planning
cable routing
deep reinforcement learning
multiple agents
variable neighborhood search
path planning.

ABSTRACT

Urban underground cable construction is essential for enhancing the reliability of city power grids, yet its high construction costs make planning a worthwhile optimization task. In urban environments, road layouts tightly constrain cable routing. This, on the one hand, renders relation-only models (i.e., those without explicit routes) used in prior work overly simplistic, and on the other hand, dramatically enlarges the combinatorial search space, thereby imposing much higher demands on algorithm design. In this study, we formulate urban cable routing as a connectivity-path co-optimization problem and propose a learning-assisted multi-operator variable neighborhood search (L-MVNS) algorithm. The framework first introduces an auxiliary task to generate high-quality feasible initial solutions. A hybrid genetic search (HGS) and A* serve as the connectivity optimizer and the route-planning optimizer, respectively. Building on these, a multi-operator variable neighborhood search (MVNS) iteratively co-optimizes inter-substation connectivity and detailed routes via three complementary destruction operators, a modified A* repair operator, and an adaptive neighborhood-sizing mechanism. A multi-agent deep reinforcement learning module is further embedded to prioritize promising neighborhoods. We also construct a standardized and scalable benchmark suite for evaluation. Across these cases, comprehensive experiments demonstrate effectiveness and stability: relative to representative approaches, MVNS and L-MVNS reduce total construction cost by approximately 30–50%, with L-MVNS delivering additional gains on larger instances and consistently higher stability.

1. Introduction

As economic development advances and reliability requirements escalate, an increasing number of cities are planning to comprehensively replace all conventional overhead lines with underground cables in their core urban areas to mitigate the impacts of extreme weather events such as typhoons and ice storms [1]. However, given the substantial costs associated with this initiative, systematically planning regional cable routing from the ground up in a cost-effective and holistic manner presents a critical optimization challenge [2].

In urban distribution systems, the segment spanning from the 110/10 kV primary substation (i.e., high-voltage (HV) substation) through the 10 kV feeders to the 10/0.4 kV distribution transformers (i.e., medium-voltage (MV) substations) constitutes the MV distribution network (DN). The associated cable infrastructure is typically designed with closed-loop feeder configurations operated in an open-loop manner, enabling back-feeding from multiple sources when required. Common layouts include interconnected and ring feeders, which can be energized from opposite ends or from a common source [3], as illustrated in Fig. 1. This arrangement supports flexible switching and maintains normal service continuity under any single-contingency $N - 1$ conditions, thereby enhancing reliability and operational resilience.

The cable routing problem is typically modeled as a combinatorial optimization problem (COP), where the goal

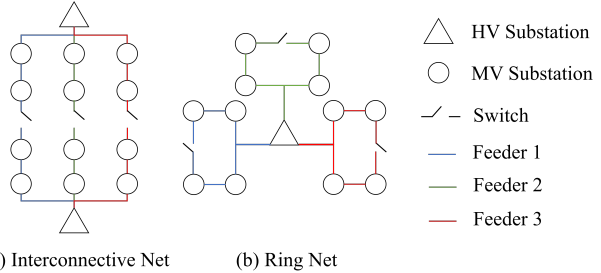


Figure 1: Typical topologies of urban MV distribution cable networks: (a) Interconnected network: MV substations are linked by feeders that originate from one HV substation and terminate at another; (b) Ring network: MV substations are linked by feeders that both originate from and terminate at the same HV substation.

is to determine the lowest-cost cable paths between substations, while satisfying capacity constraints, connection requirements, and geographical limitations. The detailed description of this problem can be found in Section 3. In contrast to cable routing challenges in wind farms and rural areas [4, 5], urban cables can only be installed beneath roads and not through existing buildings [6]. This restriction complicates decision-making in two key ways: (i) Cable Length Considerations: the feeder length between substations cannot be calculated directly by Euclidean distance, but depends on specific cable routes that strictly follow the roads; (ii) Cost Reduction through Overlapping Cables: construction costs include not just the cable procurement cost but also the

*Corresponding author

weiliu16@nudt.edu.cn (W. Liu); rui_wang@nudt.edu.cn (R. Wang)
ORCID(s): 0000-0002-6526-6526 (W. Liu)

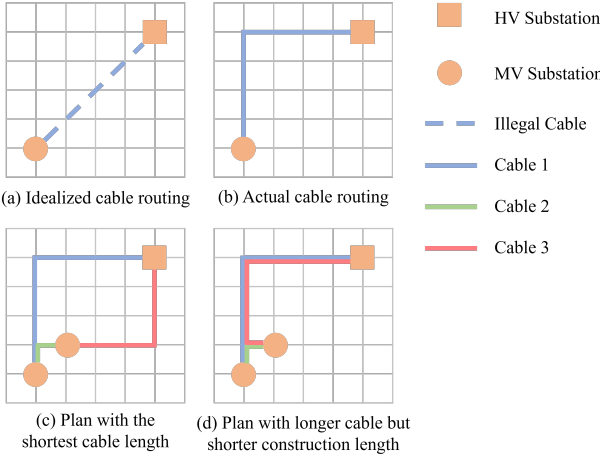


Figure 2: Schematic diagrams of the urban cable routing problem underscore two key points. First, as shown by panel (a) versus panel (b), cables cannot be laid along arbitrary straight-line segments; rather, their paths must adhere strictly to the existing road network topology. Second, as illustrated by panel (c) versus panel (d), planning multiple feeders in parallel along the same road segments can exploit spatial overlap to reduce road-trenching costs, potentially outperforming designs that rely solely on individual shortest-path routes.

road-trenching cost, which is much more expensive. Consequently, the shortest-path routing between two substations does not necessarily yield the lowest total construction cost. In many cases, deploying multiple feeders in parallel along the same road segment can reduce the total cost through overlap, even if it increases the aggregate length of cable installed [7]. Fig. 2 gives a schematic diagram to further illustrate these two points. These factors make the problem greatly complex: the decision-making space expands from $2^{N_s^2}$ to $2^{(N_r+N_s)^2}$, where N_s is the number of substations and N_r is the number of road junctions. Typically, N_r exceeds N_s by one to two orders of magnitude.

Despite decades of research on the cable routing problem, most studies have focused primarily on the connection relationships between equipment, such as substations or generators. They simplify the consideration of specific cable routes by calculating cable lengths based solely on Euclidean distances between geographic coordinates. Such simplification is typical in less congested environments, as seen in offshore wind farms [5, 8, 9, 10, 11] and old town districts [12], greatly easing problem solving. However, such simplification is not reasonable in cities, since cables are only allowed to be laid under roads. Several studies further take the geographic information system (GIS) into consideration when optimizing the cable routes [13, 14, 15, 16]. The inclusion of road information significantly complicates the problem, making it challenging to address directly with exact planning methods. As a result, dividing the original problem into multiple stages for sequential optimization paired with heuristic approaches has become a common practice [15, 7]. Instead of connecting substations directly by a straight cable,

the path planning is generally seen as an inner-layer subproblem or a second-phase sub-problem, where some classical path planning algorithms are applicable, such as the Dijkstra's algorithm [17]. A broader set of exact methods, classical heuristics, and artificial intelligence techniques has also been explored, including Benders decomposition [18], genetic algorithms [19, 20], ant colony optimization [21], neighborhood search (NS) [5], reinforcement learning [22], and imitation learning [23]. Beyond these, learning-assisted intelligent algorithms have shown substantial promise in related path-planning problems [24, 25, 26].

Section 2 describes the related literature in detail. The gaps in existing work can be concluded as follows: (i) problem modeling is overly simplified, ignoring specific cable routes linked to urban roads and the reduced road-trenching costs enabled by parallel cabling. (ii) algorithm design lacks precision, mostly relying on a multi-stage optimization with simple heuristic embedding, which is overly greedy, leading to limited optimization accuracy, especially for large-scale cases.

In this work, we reformulate the urban cable routing problem as an integrated connectivity-path co-optimization problem and construct a set of standard test instances of varying scales for evaluation. A multi-operator variable neighborhood search (MVNS) algorithm and an extra learning-assisted version (L-MVNS) are proposed to solve this problem with high precision. Within this optimization framework, an auxiliary task that integrates linear objective functions and constraints from the original problem is first formulated to enable the generation of high-quality feasible solutions. This helps improve the efficiency of subsequent searches. A hybrid genetic search (HGS) algorithm [27] combined with an A* algorithm [28] is applied here. Starting from the initial solution, MVNS iteratively co-optimizes substation interconnections and cable routes using diverse neighborhood operators: a path-related destruction operator, an inter-feeder 2-opt operator, and an intra-feeder 2-opt operator. A modified A* operator re-plans routes after destruction, and an adaptive neighborhood sizing mechanism balances exploration and exploitation. Furthermore, to handle large-scale cases, we additionally embed a multi-agent deep reinforcement learning (MDRL) model into MVNS to strategically generate the neighborhood search space, but not randomly. Each agent includes a long short-term memory network (LSTM) layer, a multi-head attention layer, and a fully connected layer. Once trained offline, these agents can autonomously define the search scope of the neighborhood operators to enhance search efficiency.

Computational experiments demonstrate the effectiveness and advantages of the proposed methods (i.e., MVNS and L-MVNS): relative to studies published in 2024, costs were reduced by approximately 30–50%. When embedded within a deep reinforcement learning (DRL) framework, MVNS not only improved solution accuracy on larger instances but also enhanced algorithmic stability. Additional parameter studies further corroborate the robustness and

scientific soundness of the approach. The main contributions of this work can be summarized as follows:

- We model urban cable routing as an integrated connectivity-path co-optimization problem that explicitly accounts for road-constrained routes and cost savings from joint-trenching. We also provide a standardized benchmark suite for algorithm evaluation.
- We construct an auxiliary optimization task that preserves parts of the objective and constraints while easing combinatorial couplings, and solve it with HGS and A*, producing strong feasible starters that accelerate subsequent search.
- We develop a multi-operator variable neighborhood search that jointly optimizes substation connections and cable routes, and employs adaptive neighborhood sizing to balance exploration and exploitation.
- We integrate a multi-agent DRL module that prioritizes promising neighborhoods and is trained offline then fine-tuned online, accelerating the search and enhancing algorithmic stability.

The remainder of this study is organized as follows: Section 2 surveys related work in detail and concludes our research motivation. Section 3 formulates the urban cable routing problem and describes benchmark construction. Section 4 presents the proposed MVNS and L-MVNS methods. Section 5 reports computational experiments on effectiveness, operator roles, and sensitivity. Section 6 concludes this study and outlines future research directions.

2. Related Work

2.1. Studies for Cable Routing

Cable routing optimization is a common task in power systems. Two prominent application domains are photovoltaic plants and wind farms, where the layout of cables connecting photovoltaic (PV) panels and wind turbines is critical for performance and cost efficiency [29, 7, 4, 5, 9]. In these relatively unobstructed environments, planners can prioritize the design of connection relationships among devices and often lay cables along near-linear paths. As a result, the problem is frequently simplified to a minimum spanning tree (MST) formulation, yielding radial network structures that satisfy electrical constraints while minimizing total cable length. A range of classical heuristics and metaheuristics has been applied in this context, including variable-depth large neighborhood search [29], Dijkstra's algorithm [4], simulated annealing, Tabu search, variable neighborhood search, ant colony optimization, and genetic algorithms [5].

However, real-world cable routing faces substantial, often non-negligible obstacles. In outdoor HV transmission, undulating terrain can significantly complicate construction, while in urban MV distribution networks, buildings

and other infrastructures may block intended routes. Consequently, it is essential to account not only for connection relationships between devices but also for the specific, feasible routing paths of the cables.

Monteiro et al. [30] and Larsson et al. [31] addressed point-to-point HV cable routing in realistic geographic settings. The former proposed a dynamic programming approach validated on small-scale case studies, highlighting an iterative and systematic procedure for optimal routing. In contrast, the latter offered a comprehensive comparison of multiple optimization techniques, including Dijkstra's algorithm, A* search, and ant colony optimization.

To interconnect urban end-users with substations operating at different voltage levels, cables must be installed strictly along designated roadways. Trageser et al. [32] transformed rendered geographic maps into cost maps and used a greedy strategy to sequence load connections, while employing the A* algorithm to compute actual route lengths. Wang et al. [15] leveraged GIS data to extract street layouts and compute shortest-path distances between substations. To manage complexity, they decomposed the task into two subproblems: closed-loop construction and open-loop operation, solving the former with the Clark–Wright Savings (CWS) heuristic and the latter with a mixed-integer linear programming (MILP) model. Pavon et al. [33] and Valenzuela et al. [34] used GIS data to formulate urban cable routing as a weighted minimum spanning tree and solved it with Prim's algorithm. [34] further applied K-means clustering for simplification. Wang et al. [35] represented the road network via a shortest-path adjacency matrix and combined Q-learning with ant colony optimization to form a multi-agent collaborative learning framework. Bosisio et al. [12] and Duvnjak et al. [36] simplified routing by optimizing only substation connections, modeling the problem as a mixed-integer program solved with commercial solvers. Table 1 summarizes the literature across several key dimensions.

2.2. Research Motivation

Nevertheless, several critical gaps remain in both the problem formulation and algorithm design.

Problem Formulation: (i) Most models oversimplify feeders as radial trees, neglecting the required single-loop, multi-source topology of urban MV grids; (ii) Length of cable routes are often simplified to the Euclidean distance between substations, but disregarding the specific routes that strictly along the roads; (iii) Cost savings from joint trenching and simultaneous installation of parallel cables are rarely accounted for.

Algorithm Design: (i) Traditional approaches often decompose the problem into sequential stages but frequently neglect how optimality constraints in earlier stages propagate to and constrain later stages, which can substantially degrade the quality of the final solution; (ii) Existing algorithms are overly simplistic and cannot reliably guarantee optimization accuracy, particularly for large-scale cases.

To address the aforementioned weaknesses, we reformulate urban cable routing as an integrated connectivity-path

Table 1

A comparative review of power cable routing methods spanning research subject, network structure, routing/overlap treatment, algorithm, and evaluation metrics. Our method appears in the final row.

Paper	Year	Research subject	Network Structure	If Cable Routes were Considered	If Cable Overlap was Considered	Algorithm ¹	Metric
[29]	2024	Photovoltaic Systems	Ring	✓	✗	VDLNS	Cost
[7]	2020	Onshore Wind Farm	Radial	✗	✓	MST	Cost
[4]	2012	Offshore Wind Farm	Radial	✗	✗	Dijkstra's MST	Distance
[5]	2020	Offshore Wind Farm	Radial	✗	✗	SA, TS, VNS, ACO, and GA	Distance
[9]	2020	Offshore Wind Farm	Radial	✗	✗	Heuristic+MIP	Distance
[30]	2005	HV DN	Radial	✓	✗	DP	Cost
[31]	2025	HV DN	Radial	✓	✗	Dijkstra, A*, and ACO	Cost and Distance
[16]	2019	LV DN	Radial	✓	✗	MILP	Cost
[32]	2022	LV DN	Radial	✓	✗	A* + Heuristic	Cost
[15]	2024	LV DN	Ring	✓	✗	CWS + MILP	Cost
[33]	2019	MV DN	Radial	✓	✗	Prim	Cost
[34]	2019	MV DN	Radial	✓	✗	K-means + Prim	Cost
[12]	2020	MV DN	2-step Ladder	✗	✗	MIP	Cost
[35]	2020	MV DN	Radial, Single Ring, and Two Supplies	✓	✗	ACO + RL + Heuristic	Cost and Reliability
[36]	2021	MV DN	Radial	✗	✗	MILP	Reliability
OURS	/	MV DN	Ring	✓	✓	HGS+A*+MVNS+MDRL	Cost

co-optimization problem that explicitly: (i) preserves the mandated single-loop, multi-source feeder architecture; (ii) restricts all cable segments to the road network; and (iii) internalizes road-trenching costs within the cost function. In parallel, we construct a suite of standardized test benchmarks of varying scales to evaluate algorithmic performance.

In terms of algorithmic design, we develop an MVNS method that jointly optimizes substation connectivity and cable routing, thereby avoiding greedy decompositions and stagewise optimization. We further formulate an auxiliary optimization task that preserves all original constraints and the key linear objective to generate a high-quality feasible initialization for MVNS, accelerating the subsequent search. Finally, an embedded multi-agent deep reinforcement learning module refines MVNS by pruning the neighborhood space and improving search efficiency. The next two sections provide a detailed description of the problem formulation and proposed method.

3. Problem and Benchmark

For clarity and consistency with our solution framework, we adopt a two-level abstraction of the cable routing problem: (i) optimizing substation connectivity at the substation-graph level, and (ii) optimizing routes that realize these connections as feasible paths at the road-graph level. The objective is to minimize total construction cost, comprising road-trenching and cable procurement.

3.1. Notation

- S_{hv} : set of HV substations (depots);
- S_{mv} : set of MV substations (customers);

- $V := S_{hv} \cup S_{mv}$: set of all substations;
- \mathcal{F} : set of feeders, indexed by f ; each feeder may start and end at the same depot or at different depots;
- $A := \{(i, j) \mid i \neq j, i, j \in V\}$: set of directed arcs between substations;
- d_{ij} : distance proxy (e.g., shortest-path length) between substations i and j ;
- q_i : contracted load (demand) at MV substation $i \in S_{mv}$ (MVA);
- Q : rated capacity of a feeder (MVA).

For Stage II (road refinement):

- $G = (\mathcal{V}, \mathcal{E})$: denotes the directed road graph extracted from GIS data, where \mathcal{V} is the set of road nodes (e.g., intersections, terminals), and \mathcal{E} is the set of directed road segments;
- ℓ_e : geometric length (km) of edge $e \in \mathcal{E}$;
- c_e^{tr} : unit road-trenching cost (million CNY/km) on edge e (CNY is Chinese Yuan);
- c_e^{ca} : unit cable-laying cost (million CNY/km) on edge e ;
- C_e^{\max} : maximum number of parallel cables permitted on edge e .

¹VDLNS: Variable Depth Large Neighborhood Search; MST: Minimum Spanning Tree; SA: Simulated Annealing; TS: Tabu Search; VNS: Variable Neighborhood Search; ACO: Ant Colony Optimization; GA:

3.2. Stage I: Connection Assignment

Decision variable (connectivity among substations)

$$x_{ij}^f \in \{0, 1\}, \quad \forall (i, j) \in A, \forall f \in \mathcal{F}, \quad (1)$$

where $x_{ij}^f = 1$ indicates that feeder f connects substations i and j .

Objective function

$$\min F_1 = \sum_{f \in \mathcal{F}} \sum_{(i, j) \in A} d_{ij} x_{ij}^f. \quad (2)$$

This stage's objective is solely to minimize total cable length.

High-level constraints Because this study does not aim to solve the problem via exact mathematical programming, and to keep the exposition concise and focused on the proposed algorithmic framework, we deliberately omit the full algebraic specification of the numerous and intricate combinatorial constraints. Instead, feasibility is encoded compactly by the abstract set \mathcal{X} :

$$\mathbf{x} \in \mathcal{X}, \quad (3)$$

which aggregates the following requirements:

- **Network topology constraint:** substation connectivity on the substation graph must conform to a ring or interconnected topology, as illustrated in Fig. 1.
- **Feeder capacity constraint:** for every feeder $f \in \mathcal{F}$, the aggregate demand of MV substations assigned to f must not exceed the feeder capacity Q .

Define the set of abstract connections retained in Stage I as

$$\mathcal{A}(\mathbf{x}) := \{(i, j, f) \in V \times V \times \mathcal{F} \mid x_{ij}^f = 1\}, \quad (4)$$

it constitutes the input pairs for Stage II.

3.3. Stage II: Route Refinement

Stage II implements the abstract connections $\mathcal{A}(\mathbf{x})$ on the road graph by choosing which edges to excavate and how many parallel cables to place on each.

Decision variables (connectivity on the road graph)

$$y_e \in \{0, 1\}, \quad k_e \in \{0, 1, \dots, C_e^{\max}\}, \quad \forall e \in \mathcal{E}, \quad (5)$$

where $y_e = 1$ denotes that edge e is excavated (used), and k_e is the number of parallel cables laid on e .

Genetic Algorithm; **MIP**: Mixed Integer Programming; **DP**: Dynamic Programming; **MILP**: Mixed Integer Linear Programming; **CWS**: Clark-Wright Savings Algorithm; **Prim**: Prim's Algorithm; **K-means**: K-means Clustering Algorithm; **RL**: Reinforcement Learning; **HGS**: Hybrid Genetic Search; **MVNS**: Multi-operator variable neighborhood search; **MDRL**: Multi-agent Deep Reinforcement Learning.

Objective function

$$\min F_2 = \sum_{e \in \mathcal{E}} \left(c_e^{\text{tr}} \ell_e y_e + c_e^{\text{ca}} \ell_e k_e \right). \quad (6)$$

This stage's objective considers both cable procurement and road-trenching costs.

High-level constraints feasibility is encoded by a set $\mathcal{Y}(\mathcal{A}(\mathbf{x}))$:

$$(\mathbf{y}, \mathbf{k}) \in \mathcal{Y}(\mathcal{A}(\mathbf{x})), \quad (7)$$

which encompasses:

- **Connectivity realization:** for every abstract link $(i, j, f) \in \mathcal{A}(\mathbf{x})$, the nodes associated with substations i and j are connected by a path in the subgraph induced by $\{e \in \mathcal{E} : y_e = 1\}$.
- **Trenching-cabling consistency:** cables are laid only on excavated edges (trenching can be shared across multiple cables).

3.4. Integrated Formulation

The problem can be cast as a mixed-integer program that minimizes the construction cost F_2 while coupling connectivity and routing:

$$\begin{aligned} \min & F_2(S) \\ \text{s.t.} & \mathbf{x} \in \mathcal{X}, \\ & (\mathbf{y}, \mathbf{k}) \in \mathcal{Y}(\mathcal{A}(\mathbf{x})), \end{aligned} \quad (8)$$

where $S = (\mathbf{x}, \mathbf{y}, \mathbf{k})$ represents the solution, with $x_{ij}^f \in \mathbf{x}$, $y_e \in \mathbf{y}$, and $k_e \in \mathbf{k}$.

Given $|\mathcal{F}|$ feeders, $|A|$ candidate substation arcs, and $|\mathcal{E}|$ road edges, there are $|\mathcal{F}||A| + 2|\mathcal{E}|$ binary variables, often surpassing 10^6 for typical urban settings. The resulting formulation is tightly constrained by structural and capacity requirements, rendering it a large-scale, multi-constraint combinatorial optimization problem that lies beyond the practical capabilities of standard exact MIP solvers.

3.5. Benchmark Construction

To evaluate algorithms in a controllable yet scalable setting, we construct a suite of test instances on regular square lattices. The grid size governs instance scale, while the orthogonal geometry approximates block street layouts. An $n_{\text{grid}} \times n_{\text{grid}}$ lattice represents n_{grid}^2 uniformly aligned blocks, each 1 km \times 1 km. HV and MV substations are generated via a two-level clustering procedure. First, each lattice node is treated as a load aggregation point, and K-means partitions all nodes into N_{mv} clusters; their centroids define candidate MV substations. Second, the MV centroids are reclustered into N_{hv} groups to obtain HV substations. Because a centroid may not coincide with a lattice vertex, we project each centroid to the closest point on the nearest lattice edge.

Following the literature [37, 38], we adopt the following parameterization: the peak demand q_i at each MV substation i is drawn uniformly from [2, 5] MVA with sufficient redundancy. Each feeder has a rated capacity of $Q = 10$ MVA. The maximum number of parallel cables per edge is $C_e^{\max} = 6$. Unit costs are set to 1.5 million CNY/km for road trenching (c_e^{tr}) and CNY 0.5 million CNY/km for cable laying on edge e (c_e^{ca}). With random seed 42, we generate four scales and Fig. 3 visualizes them.

- Case-1: 20×20 grid, $N_{mv} = 30$, $N_{hv} = 5$;
- Case-2: 30×30 grid, $N_{mv} = 50$, $N_{hv} = 6$;
- Case-3: 30×30 grid, $N_{mv} = 80$, $N_{hv} = 7$;
- Case-4: 30×30 grid, $N_{mv} = 100$, $N_{hv} = 8$.

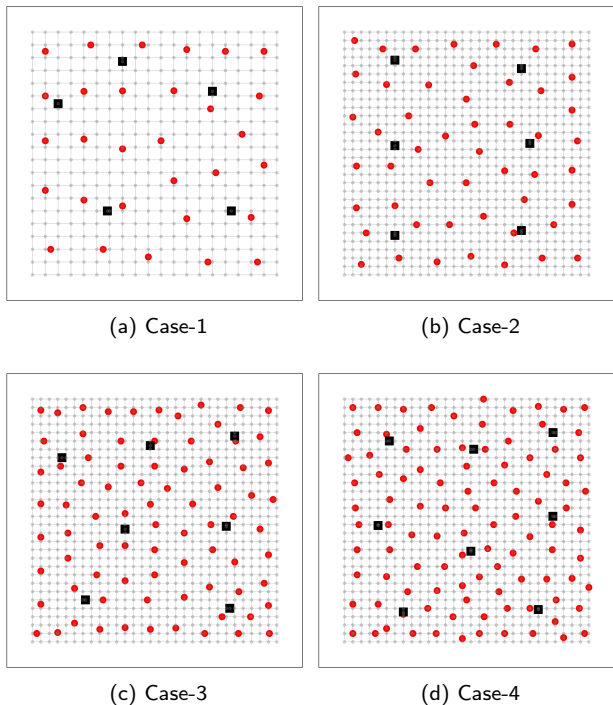


Figure 3: Street layouts and substations for the four built cases, with HV substations as black squares and MV substations as red points.

4. Proposed Method

Fig. 4 presents the overall architecture of the proposed L-MVNS algorithm, which consists of three modules: (i) **Solution Initialization**: an auxiliary task is constructed and solved through a connection–relationship optimizer and a route–planning optimizer to quickly produce a high-quality, feasible initial solution. (ii) **Learning-Assisted Neighborhood Generation**: three DRL agents are pre-trained offline and, online, generate the neighborhood search space for a given neighborhood operator. (iii) **Multi-operator**

Variable Neighborhood Search: three complementary operators jointly optimize substation connections and cable routing: a path-oriented destruction operator, an inter-feeder 2-opt operator, and an intra-feeder 2-opt operator. A modified A* algorithm replans detailed connection paths between substations. Unlike conventional variable neighborhood search methods, which adaptively select a single neighborhood search operator, our MVNS adaptively adjusts the neighborhood scope of multiple collaborative neighborhood operators. Further details of these modules are provided in the following subsections.

4.1. Auxiliary Task Construction for Solution Initialization

We first formulate an auxiliary optimization problem that uses only inter-substation shortest-path distances, omitting explicit cable-routing decisions. In other words, we solve Stage I as defined in Section 3.2 and defer road-constrained routing to a subsequent module. This problem is tackled with a two-step pipeline that sequentially optimizes the connection topology among substations and the point-to-point shortest paths for the selected pairs.

This design decomposes the original co-optimization into two well-studied combinatorial subproblems for which state-of-the-art solvers are readily available. Specifically, we cast the connection-relationship optimization as a multi-depot capacitated vehicle routing problem (MD-CVRP) over the substation set, using road-graph shortest-path distances as arc costs. We solve this subproblem with the HGS algorithm [39, 27], a leading metaheuristic for vehicle-routing variants known for robust performance and rapid convergence. Given the resulting feeder-level connection pairs, we then compute the corresponding point-to-point routes via the A* algorithm [28] on the road graph, ensuring path optimality under the chosen edge metrics.

While this auxiliary solution is typically high quality and computationally efficient, it does not coincide with the true optimum of the original problem. The gap arises because the simplification ignores potential savings in road-trenching costs from joint trenching and parallel cable placement along shared edges. In the proposed framework, however, this initialization serves as a feasible anchor that is subsequently refined by the MVNS operators.

4.2. Multi-operator Variable Neighborhood Search Method

The proposed MVNS procedure iteratively destroys and repairs a feasible solution to jointly optimize feeder connections and detailed routes. As summarized in Algorithm 1, each iteration comprises three stages: (i) adaptive perturbation sizing based on the stagnant times (line 3); (ii) destruction location generation via random sampling (line 7) and neighborhood exploration via sequentially applying three complementary destruction operators, each followed by a unified repair routine \mathbb{R} and cost evaluation \mathbb{E} (lines 5–13); and (iii) best-candidate acceptance with stagnation-aware diversification (lines 14–19).

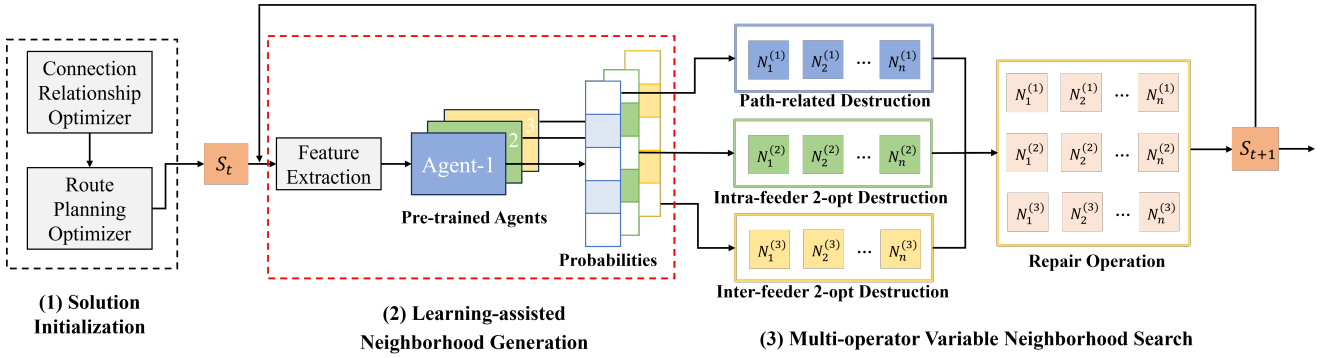


Figure 4: The proposed L-MVNS algorithm comprises three modules: solution initialization, learning-assisted neighborhood generation, and multi-operator variable neighborhood search. The final solution is iteratively refined in the latter two modules.

Concretely, at iteration t , the algorithm uses perturbation size κ to sample N candidates per destruction operator from the current solution S . κ is adaptively set by the stagnation counter st (line 3). For each candidate, the destruction locations \mathcal{L} is drawn via random sampling $SampleLocs(S, \kappa)$ (line 7). The destruction operator \mathbb{D} then partially removes or reconfigures elements of S over \mathcal{L} , yielding an intermediate solution \hat{S} (line 8). The repair operator \mathbb{R} restores feasibility and exploits trench-sharing opportunities by re-planning paths between substations (line 9). The evaluation operator \mathbb{E} computes the total cost \hat{C} of the repaired solution (line 10), as defined in Equation (6). Among all candidates synthesized across operators, the algorithm selects the best-scoring solution (\hat{S}, \hat{C}) (line 14). If $\hat{C} < C^*$, the incumbent is updated and the stagnation counter is reset, biasing subsequent iterations toward intensification around the new incumbent (line 16). Otherwise, the stagnation counter is incremented (line 18). The resulting increase in κ enlarges the destruction scope in future iterations, promoting broader exploration of the search space.

Below we detail the involved operators and functions. Fig. 5 illustrates the operational schematics of the three destruction operators: $\mathbb{D}^{(1)}$, $\mathbb{D}^{(2)}$, and $\mathbb{D}^{(3)}$. These operators do not determine the specific post-destruction routes; those routes are re-planned by the repair operator \mathbb{R} and the costs are evaluated by the evaluate operator \mathbb{E} .

- $\mathbb{D}^{(1)}$: path-related destruction, which randomly removes feeder paths between κ pairs of interconnected substations.
- $\mathbb{D}^{(2)}$: intra-feeder 2-opt destruction, which selects two non-adjacent edges (between substations) along the same feeder's substation sequence and performs a 2-opt recombination. That is, it reverses the intervening path segment between the selected edges to yield a new, potentially shorter, route configuration.
- $\mathbb{D}^{(3)}$: inter-feeder 2-opt destruction, which selects two distinct feeders and one edge (between substations) on each, then exchanges the corresponding route segments.

Algorithm 1 Multi-operator Variable Neighborhood Search Method (MVNS)

Input: Initial solution S with cost C , case graph G , neighborhood size N , max iterations $Iterations$

Output: Best solution S^* with costs C^*

1: Set $S^* \leftarrow S, C^* \leftarrow C, st \leftarrow 0$

```

2: for  $t = 1$  : Iterations do
3:    $\kappa \leftarrow SetKappa(st)$             $\triangleright$  Perturbation size
4:    $CS \leftarrow \emptyset$        $\triangleright$  Initialize the candidate solution set
5:   for  $neighbor = 1$  :  $N$  do
6:     for  $\mathbb{D} \in \{\mathbb{D}^{(1)}, \mathbb{D}^{(2)}, \mathbb{D}^{(3)}\}$  do
7:        $\mathcal{L} \leftarrow SampleLocs(S, \kappa)$      $\triangleright$  Generate the
         destruction locations
8:        $\tilde{S} \leftarrow \mathbb{D}(S, \mathcal{L})$            $\triangleright$  Destruction operator
9:        $\tilde{S} \leftarrow \mathbb{R}(\tilde{S}, G)$            $\triangleright$  Repair operator
10:       $\tilde{S}, \tilde{C} \leftarrow \mathbb{E}(\tilde{S}, G)$        $\triangleright$  Evaluate operator
11:       $CS \leftarrow CS \cup \{(\tilde{S}, \tilde{C})\}$ 
12:    end for
13:  end for
14:   $(\hat{S}, \hat{C}) \leftarrow \arg \min_{(S', C') \in CS} C'$ 
15:  if  $\hat{C} < C^*$  then
16:     $S^* \leftarrow \hat{S}, S \leftarrow \hat{S}, C^* \leftarrow \hat{C}, st \leftarrow 0$ 
17:  else
18:     $st \leftarrow st + 1$ 
19:  end if
20: end for
21: return  $S^*, C^*$ 

```

- \mathbb{R} : unified route re-planning, which restores feasibility in a partially disrupted solution by reconnecting all affected terminal pairs on the road graph using a modified A* algorithm. In its standard form, A* evaluates neighbors via $f(n) = g(n) + h(n)$, where $g(n)$ is the exact cost from the start to node n and $h(n)$ is an evaluated cost from n to the goal. In our approach, $h(n)$ is defined as the Manhattan distance and $g(n)$ is revised to include trench-sharing and cable-placement costs, as in Equation (6), thereby encouraging lower total cost through the deployment of parallel cables

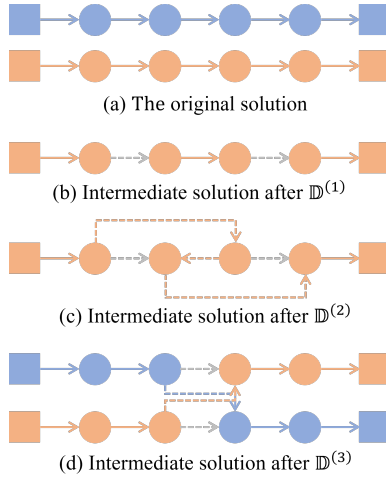


Figure 5: The operation diagrams for the three destruction operators: squares indicate HV substations, circles denote MV substations, orange and blue modules signify two independent feeders, gray dotted lines represent removed segments, and orange and blue dotted lines represent newly connected segments.

along shared edges. When multiple routes require re-planning, their processing order is randomized.

- \mathbb{E} : cost evaluation function, which computes the objective by aggregating cable-length and trench-construction costs over edges, as defined in Equation (6).
- *SetKappa*: adaptive perturbation function, that incrementally adjusts the perturbation size κ according to the number of stagnation occurrences st , as in Equation (9). This scheme balances exploitation (smaller κ when improving) and exploration (larger κ under stagnation) during iteration.

$$\kappa(st) = \begin{cases} 2, & \text{if } st < 20, \\ 4, & \text{if } 20 \leq st < 30, \\ 6, & \text{if } 30 \leq st < 40, \\ 8, & \text{if } st \geq 40. \end{cases} \quad (9)$$

4.3. Multi-Agent Deep Reinforcement Learning for Improvement

Although the aforementioned MVNS method is available for generating good solutions, the exponential growth of its search space in large-scale instances makes efficient identification of the optimum challenging. To address this, we embed a multi-agent deep reinforcement learning model within MVNS. At each iteration, the model autonomously constructs the neighborhood search space based on the current state, replacing simple random sampling and thereby accelerating convergence. We refer to this learning-assisted variant as L-MVNS. To preserve exploration and reduce the risk of premature convergence, neighborhoods are generated

by pre-trained agents with the probability of 70% and selected at random with the probability of 30%.

Each DRL agent is paired with a designated destruction operator and ingests features of the current best solution to output, for every edge, its probability of being selected for destruction. Using this probability vector, we perform weighted sampling to construct the set of edges to remove, thereby replacing the prior uniform random sampling in the MVNS framework (i.e., line 7, $\mathcal{L} \leftarrow \text{SampleLocs}(S, \kappa)$, in Algorithm 1). This procedure determines the gray dotted boundary in Fig. 5 and yields N candidate solutions within the induced neighborhood, as illustrated in the second module of Fig. 4.

In this learning task (see Fig. 6), each agent's state s_t encodes the current best solution at iteration t as a three-dimensional tensor of shape $E \times M \times D$. Here, E is the number of substation-to-substation paths, M is the maximum number of nodes per path (including road nodes), and $D = 2$ stores the planar coordinates of nodes. The action a_t specifies the perturbation applied to the incumbent solution, that is, the set of edges to destroy. a_t is obtained by probability sampling from the probability vector $p(a | s_t)$ produced by the neural network.

After the destroyed edges are re-planned via the repair operator \mathbb{R} , the reward r_t provides feedback on action quality and is defined as follows:

$$r_t = \begin{cases} \frac{C_t^* - C_{t+1}}{C_t^*}, & \text{if } C_{t+1} < C_t^*, \\ 0, & \text{otherwise,} \end{cases} \quad (10)$$

where C_{t+1} is the cost of the new solution, and C_t^* is the minimum cost found so far.

During training, each agent employs a policy $p(a | s)$ that maps states to actions. After accumulating per-sample losses over a batch, the policy network parameters are updated by minimizing the aggregated loss L :

$$L = -\frac{1}{B} \sum_{i=1}^B (r_i - b(s_i)) \log p(a_i | s_i; \theta), \quad (11)$$

where B is the batch size, r_i is the reward for action a_i , s_i is the corresponding state, and $b(s_i)$ is a baseline function that reduces variance in the reward signal. The baseline $b(s_i)$ is evaluated by a three-layer fully connected neural network.

As shown in Fig. 6, each agent comprises three components: (i) an LSTM module to capture sequential dependencies within a single cable feeder; (ii) a multi-head attention module to model spatial interactions across different feeders; and (iii) a two-layer fully connected module for regression that outputs a probability vector $p(s_i)$. The outputs of LSTM and attention are combined via a residual connection to preserve sequential features and stabilize training. All hidden sizes are set to 64, and the attention module uses 2 heads. Further details on LSTM and multi-head attention can be found in [40] and [41]. The network parameters θ

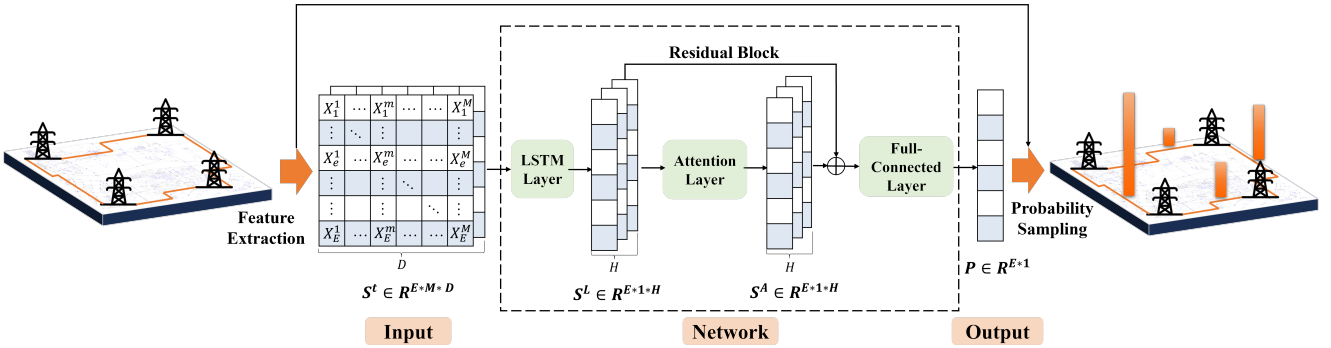


Figure 6: Schematic of the neural network architecture and feedforward computation. Each agent comprises a sequential stack of an LSTM layer, a multi-head attention layer, and a fully connected layer. The network ingests a three-dimensional tensor that encodes the two-dimensional coordinates of all nodes along the routes in the current best solution. The output is a probability vector over existing edges indicating their likelihood of destruction. By repeatedly performing probability sampling from this probability vector, the model generates a set of structurally perturbed solutions (i.e., neighborhood solutions).

are updated through gradient descent, as formulated below:

$$\theta \leftarrow \theta - \alpha \nabla L, \quad (12)$$

where α is the learning rate.

5. Experiments and Results

Experiments were conducted on a PC equipped with an AMD Ryzen 7 5800H CPU (3.2 GHz) and an NVIDIA GeForce RTX 3060 GPU. The source code will be released upon publication of the paper. The following sections detail the model training, effectiveness comparison, operator function, and sensitivity analysis.

5.1. Model Training

In our training setup, we adopt a two-stage method comprising offline pretraining followed by brief online fine-tuning. Specifically, the three agents are first pretrained on a small-scale instance (Case-0: 20×20 grid, $N_{mv} = 20$, $N_{hv} = 4$). The training data comprise triples (s_t, s_{t+1}, r_t) collected from MVNS search trajectories on Case-0, using a neighborhood size of 10 per operator and a maximum of 2000 iterations. We train for up to 50 epochs with mini-batches of size $B = 32$ and an initial learning rate $\alpha = 1 \times 10^{-4}$, employing a 10% warmup schedule. Pretraining requires approximately 2 hours.

For online adaptation on each target instance, we leverage data from the first 200 iterations to perform transfer learning under the same hyperparameter configuration, enabling rapid case-specific calibration without modifying the backbone architecture.

Fig. 7 reports the reward curves for the multi-agent aggregation model and each of the three individual agents during training. The reward, defined in Equation (10), measures the proportion of the total cost reduced by a single neighborhood-search iteration. Across runs, the rewards display a clear convergence trend, indicating that the model

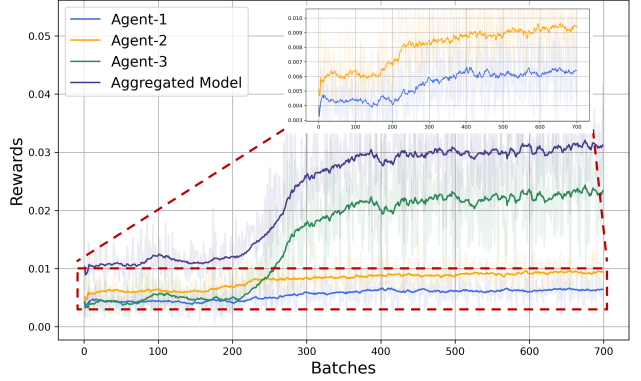


Figure 7: Reward curves of the multi-agent aggregation model and individual agents are shown during training: the shadow curves represent original data and the opaque curves represent smoothed data (window size = 30).

parameters are being effectively learned. Notably, Agent-3 achieves higher rewards than Agent-1 and Agent-2 after training, indicating that its strategy parameter updates yield greater performance gains.

5.2. Effectiveness Comparison

To evaluate the proposed method, we benchmark two classes of algorithms on the test instances: (i) relation-only baselines that optimize substation connectivity using precomputed shortest-path distances while ignoring explicit trench sharing, thereby equating trench length with cable length. This is the most common approach in traditional research, such as the modified two-phase Clark-Wright savings algorithm (**MCWS**) [15], which was proposed in 2024. In addition to this, we formulate the original problem as a multi-depot vehicle routing problem and solve it with **HGS** [39], which matches the initialization phase of our framework; (ii) path-aware baselines that explicitly model

Table 2

Effectiveness comparison of relation-only baselines (MCWS and HGS) and path-aware methods (SNS-1/2/3, MVNS, and L-MVNS) across four cases. For each method, results over 10 independent runs include mean cost (million CNY), variance, and the percentage gap to the best competing method. Best values are highlighted in gray.

Method	Case-1			Case-2			Case-3			Case-4		
	Mean	Var	Gap(%)	Mean	Var	Gap(%)	Mean	Var	Gap(%)	Mean	Var	Gap(%)
MCWS	3787.80	0.00	52.65	8602.80	0.00	62.66	13765.80	0.00	99.17	16020.20	0.00	99.52
HGS	3244.40	0.00	30.75	6716.00	0.00	26.98	9889.60	0.00	43.09	11386.60	0.00	41.82
SNS-1	2559.75	1786.28	3.16	5325.11	3494.07	0.68	7130.63	2000.97	3.17	8193.06	4232.74	2.04
SNS-2	2582.91	3015.25	4.09	5527.26	1694.81	4.51	7253.22	3063.31	4.94	8248.72	4555.78	2.73
SNS-3	2535.95	2782.67	2.20	5570.78	3285.46	5.33	7464.54	4999.30	8.00	8433.52	14282.30	5.04
MVNS	2481.42	4027.43	0.00	5295.26	2246.12	0.12	7015.43	2758.93	1.50	8043.41	4306.97	0.18
L-MVNS	2489.23	16.67	0.31	5288.96	1537.89	0.00	6911.53	680.51	0.00	8029.18	646.54	0.00

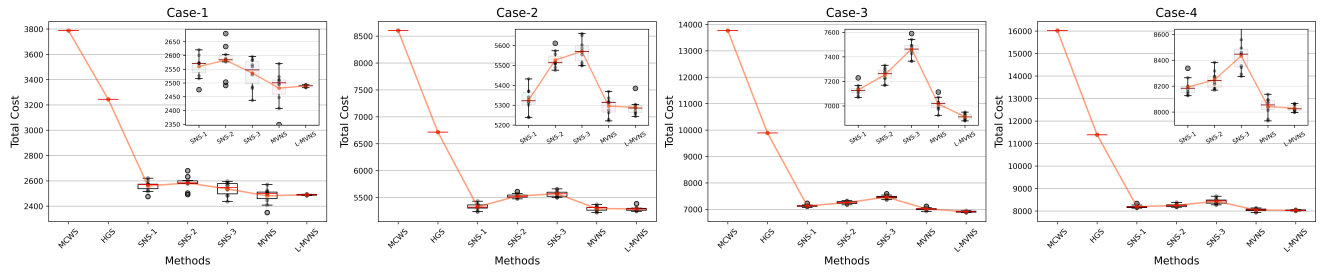


Figure 8: Boxplots of solution costs for all methods on Cases 1–4 over 10 independent runs. Boxes show the interquartile range with median lines; whiskers indicate non-outlier ranges; red points mark the mean and are connected across methods. Lower values indicate better performance. For clarity, SNS-1/2/3, MVNS, and L-MVNS are also displayed as separate subplots.

cable paths and trench sharing, including three single-neighborhood search methods in our framework (i.e., **SNS-1**, **SNS-2**, and **SNS-3**, respectively utilizing the destruction operators $\mathbb{D}^{(1)}$, $\mathbb{D}^{(2)}$, and $\mathbb{D}^{(3)}$), the proposed **MVNS**, and the proposed **L-MVNS**. For fair comparison, SNS-1, SNS-2, and SNS-3 use a neighborhood size of 30, while MVNS and L-MVNS use 10 per operator (three operators, totaling 30). The maximum number of iterations for all neighborhood search methods is set to 600.

Each algorithm was evaluated using 10 independent runs per test case. Table 2 reports the mean solution cost across runs, the variance, and the percentage gap relative to the best competing algorithm. Best values are highlighted in gray. Fig. 8 further presents boxplots of the costs across the 10 runs.

The analysis of these experimental results is presented from the following perspectives:

5.2.1. Path-aware Baselines versus Relation-only Baselines

Path-aware baselines (SNS-1, SNS-2, SNS-3, MVNS, and L-MVNS) reduce costs by approximately 30–50% relative to relation-only baselines (MCWS and HGS). The savings arise because the unit cost of road trenching typically exceeds that of cable by a large margin, about threefold in engineering practice [7]. This finding underscores the value of explicitly modeling actual cable routing paths and trench sharing in planning. Fig. 9 presents representative solutions produced by HGS and L-MVNS across the four

cases. It is evident that, through iterative optimization with L-MVNS, both the inter-substation connectivity and the specific route choices change substantially. In particular, the parallel placement of multiple cables along shared routes (i.e., the darker lines) markedly reduces overall cost.

5.2.2. HGS versus MCWS

Although MCWS is a representative approach for urban cable planning, its optimization accuracy leaves substantial room for improvement. The gap primarily stems from two factors: (i) the decomposition of the original problem into a multi-stage, sequential process, where early decisions may exclude globally optimal solutions later; and (ii) the use of greedy heuristics for each subproblem (e.g., sweep rules for clustering substations and the Clarke–Wright savings algorithm for intra-cluster sequencing), which inherently limits solution quality. By contrast, modeling the original problem as an MD-CVRP and solving it globally with a state-of-the-art algorithm (HGS) yields substantially better solutions.

5.2.3. Multiple Neighborhood Search versus Single Neighborhood Search

Under identical experimental settings, the multi-neighborhood search methods (MVNS and L-MVNS) outperform the single-neighborhood search methods (SNS-1/2/3) by a clear margin. Although each operator in SNS explores a larger neighborhood (30) than that in MVNS (10), a single operator cannot simultaneously refine inter-node connectivity

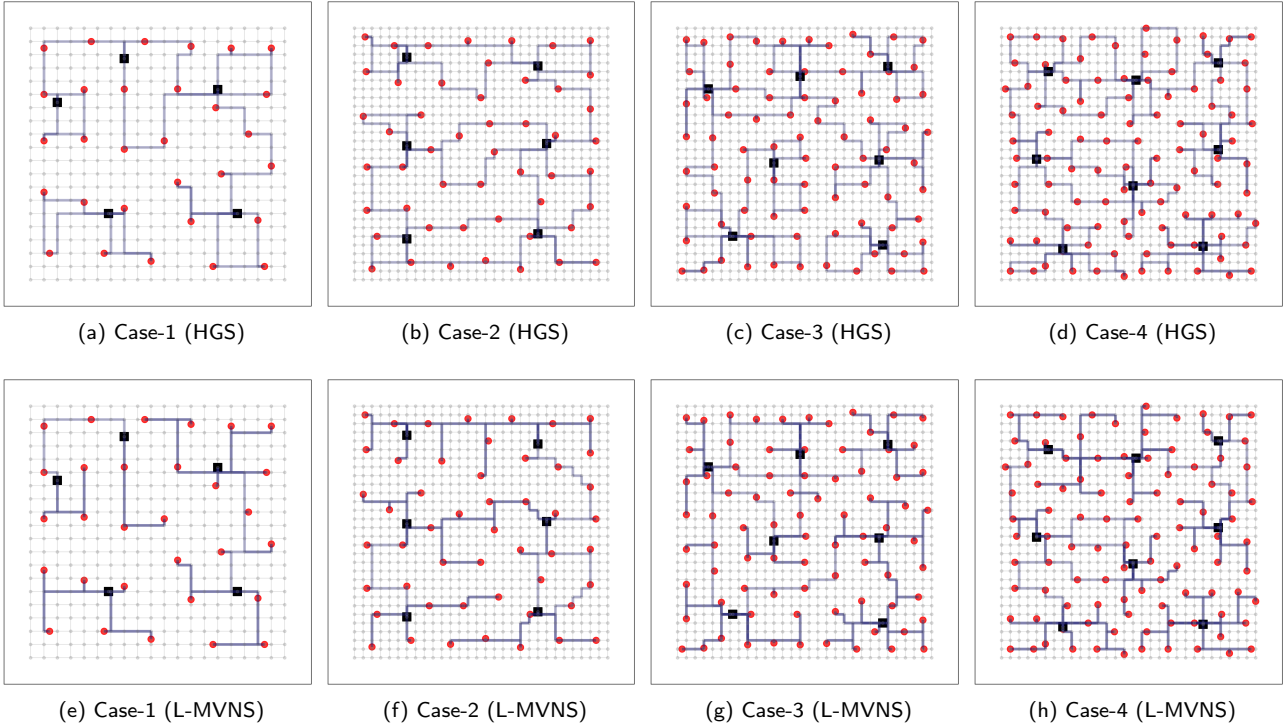


Figure 9: Representative solutions for Cases 1–4 obtained by HGS (top row) and L-MVNS (bottom row). L-MVNS substantially adjusts both substation connectivity and route choices, with parallel cable placement along shared trenches (darker lines) reducing total cost.

and specific routing paths within the incumbent solution, hindering progress toward global optimality.

5.2.4. L-MVNS versus MVNS

The last two rows of Table 2 report the performance of the proposed MVNS and L-MVNS across all cases. Both methods achieve higher accuracy than competing algorithms: MCWS shows gaps of 52%–100%, HGS 27%–42%, and SNS-1/2/3 1%–8%. The differences between MVNS and L-MVNS are modest overall, with L-MVNS slightly outperforming MVNS on the large-scale cases (Cases 2–4). This likely reflects that more complex instances provide richer data for transferring and refining model parameters. Beyond accuracy improvement, incorporating DRL in L-MVNS consistently reduces variance across independent runs. This stability gain arises because MVNS selects neighborhoods uniformly at random, whereas L-MVNS samples neighborhoods according to probabilities produced by the DRL component, thereby providing informed guidance during the search.

5.3. Operator Function

Fig. 10 presents a further statistical analysis of the roles played by the three neighborhood search operators during the search processes of MVNS and L-MVNS, quantified by the number of times each operator generated the next locally optimal solution. According to this statistical result, the neighborhood operator-1 (i.e., the path-related destruction operator) appears more frequently than the other two

operators. Consistent with this, Fig. 8 shows that SNS-1 achieves higher optimization accuracy than SNS-2 and SNS-3. This outcome is expected: the initial solution used for neighborhood search typically already exhibits reasonable connectivity, leaving the primary room for improvement in reducing road-trenching costs via parallel cable deployment, which is precisely the focus of the operator-1. Nonetheless, because connectivity optimization and route refinement are inherently coupled subproblems, the operator-2 (i.e., the inter-feeder 2-opt operator) and the operator-3 (i.e., the intra-feeder 2-opt operator) still make meaningful contributions during the optimization process.

5.4. Sensitivity Analysis

This subsection examines how two key hyperparameters affect MVNS performance: (i) initialization time allocated to the auxiliary task and (ii) neighborhood size per destruction operator. We report impacts on solution quality, runtime, and stability across the medium-scale test case: Case-3.

5.4.1. Initialization time

We varied the initialization (i.e., auxiliary task optimization) time from 10 to 600 seconds to assess its impact on the subsequent search. The maximum iteration count is fixed at 400. Fig. 11 reports MVNS performance on Case-3 over 10 independent runs for each initialization time. In general, longer initialization yields faster convergence during the neighborhood search; however, beyond 200 seconds, the

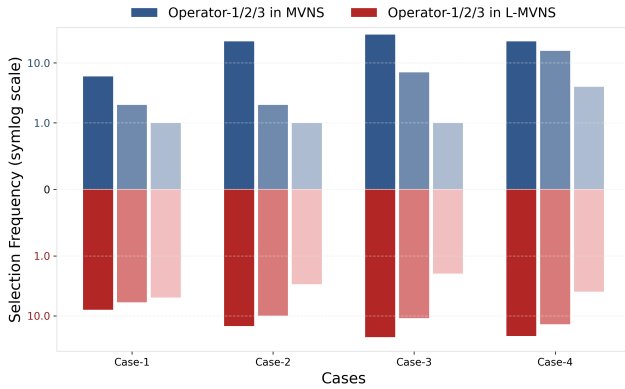


Figure 10: Statistical comparison of the three neighborhood operators (i.e., $\mathbb{D}^{(1)}$, $\mathbb{D}^{(2)}$, and $\mathbb{D}^{(3)}$) used in MVNS and L-MVNS, measured by the number of times each operator produced the next locally optimal solution. Blue bars denote operator frequencies in MVNS across all cases; red bars denote the corresponding frequencies in L-MVNS. The y-axis uses a logarithmic scale to enable clearer cross-scale comparison.

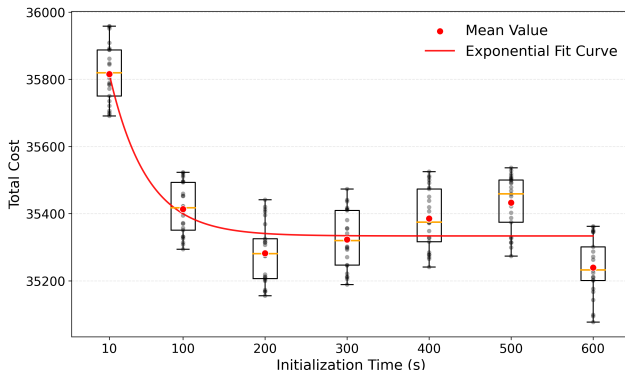


Figure 11: Boxplots of MVNS performance on Case-3 over 10 runs with initialization time from 10 to 600 seconds. Red dots (mean values) follow an approximate decaying-exponential trend.

marginal reduction in total cost plateaus. The mean performance at each initialization time (i.e., red dots) approximately follows a decaying exponential trend. Notably, in fact, a longer initialization does not necessarily produce a better initial solution because the auxiliary task does not explicitly account for road-trenching costs. Accordingly, we set the initialization time to 200 seconds, as allocating more time offers limited returns.

5.4.2. Neighborhood size

Expanding the neighborhood search range can improve the likelihood of reaching a global optimum, but it also increases computational cost and runtime. In this subsection, we evaluate MVNS under different neighborhood sizes to identify a suitable trade-off. We vary the number of candidate sizes per operator N from 5 to 25 (so MVNS explores $3N$ neighborhoods per iteration). Fig. 12 reports MVNS

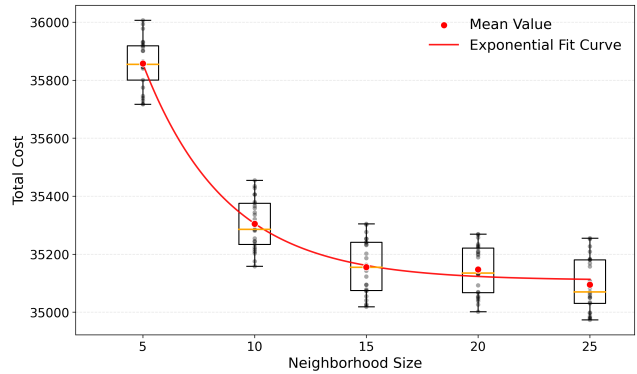


Figure 12: Boxplots of MVNS performance on Case-3 over 10 runs with neighborhood size per operator from 5 to 25. Red dots (mean values) follow an approximate decaying-exponential trend.

performance on Case-3 across 10 independent runs for each setting.

The average cost drops markedly when increasing N from 5 to 10. Beyond $N = 15$, solution quality plateaus while runtime grows linearly with N . Moreover, very large neighborhoods can dilute the benefits of DRL guidance because the acceptance pool increasingly includes low-quality, randomly perturbed candidates. Therefore, balancing accuracy and efficiency, we set the neighborhood size per operator to 10.

6. Conclusion

Regarding the urban cable routing problem, this paper formulates it as an integrated connectivity–path co-optimization problem that explicitly accounts for road-constrained routing and cost savings from joint trenching. Building on this formulation, we propose a learning-assisted multi-operator variable neighborhood search (L-MVNS) framework that jointly optimizes substation connectivity and detailed cable routes. The method starts from a high-quality initial solution derived via an auxiliary MD-CVRP subproblem solved with HGS and A*, then applies a destroy-and-repair process featuring three destruction operators, a unified repair operator, and an adaptive neighborhood sizing mechanism. To scale to large instances, we embed multi-agent deep reinforcement learning that produces state-aware neighborhoods, accelerating convergence and improving stability. Extensive experiments across four benchmarks show that path-aware methods substantially outperform relation-only baselines. Compared with representative 2024 approaches, our methods reduce total construction costs by approximately 30–50%. MVNS and L-MVNS consistently yield the best solutions, with L-MVNS delivering additional gains on larger instances and lower variance across independent runs.

Future work will extend the framework to multi-objective optimization with reliability considerations and outage penalties under stochastic failures. In parallel, fully leveraging deep reinforcement learning to augment neighborhood

search remains a promising yet challenging direction. The key challenge is to improve the agent's learning efficiency and generalization so that it adapts robustly across diverse problem instances and operational conditions.

References

- [1] Zhou, Y.. Low-carbon urban-rural modern energy systems with energy resilience under climate change and extreme events in china—a state-of-the-art review. *Energy and Buildings* 2024;114661.
- [2] Milošević, N.D., Popović, Ž.N., Kovački, N.V.. A multi-period multi-criteria replacement and rejuvenation planning of underground cables in urban distribution networks. *International Journal of Electrical Power & Energy Systems* 2023;149:109018.
- [3] Diaz-Dorado, E., Cidrás, J., Míguez, E.. Application of evolutionary algorithms for the planning of urban distribution networks of medium voltage. *IEEE Transactions on Power Systems* 2002;17(3):879–884.
- [4] Dutta, S., Overbye, T.J.. Optimal wind farm collector system topology design considering total trenching length. *IEEE Transactions on Sustainable Energy* 2012;3(3):339–348.
- [5] Cazzaro, D., Fischetti, M., Fischetti, M.. Heuristic algorithms for the wind farm cable routing problem. *Applied Energy* 2020;278:115617.
- [6] Bai, Y., Zhou, R., Wu, J.. Hazard identification and analysis of urban utility tunnels in china. *Tunnelling and Underground Space Technology* 2020;106:103584.
- [7] Deveci, K., Barutçu, B., Alpman, E., Taşçıkaraoğlu, A., Erdinç, O.. Electrical layout optimization of onshore wind farms based on a two-stage approach. *IEEE Transactions on Sustainable Energy* 2019;11(4):2407–2416.
- [8] Cazzaro, D., Koza, D.F., Pisinger, D.. Combined layout and cable optimization of offshore wind farms. *European Journal of Operational Research* 2023;311(1):301–315.
- [9] Ulku, I., Alabas-Uslu, C.. Optimization of cable layout designs for large offshore wind farms. *International Journal of Energy Research* 2020;44(8):6297–6312.
- [10] Wu, Y., Zhang, S., Wang, R., Wang, Y., Feng, X.. A design methodology for wind farm layout considering cable routing and economic benefit based on genetic algorithm and geostainer. *Renewable Energy* 2020;146:687–698.
- [11] Tao, S., Jiang, F., Yang, J., Feijoo-Lorenzo, A.E.. Optimal cabling of deep-sea far-shore wind farm considering complex seabed and restricted zones. *IEEE Transactions on Industrial Informatics* 2025;21(7):5557–5568.
- [12] Bosisio, A., Berizzi, A., Amaldi, E., Bovo, C., Sun, X.A.. Optimal feeder routing in urban distribution networks planning with layout constraints and losses. *Journal of Modern Power Systems and Clean Energy* 2020;8(5):1005–1014.
- [13] Bosisio, A., Berizzi, A., Bovo, C., Amaldi, E., Fratti, S.. Gis-based urban distribution networks planning with 2-step ladder topology considering electric power cable joints. In: 2018 AEIT International Annual Conference. IEEE; 2018, p. 1–6.
- [14] Bosisio, A., Berizzi, A., Amaldi, E., Bovo, C., Morotti, A., Greco, B., et al. A gis-based approach for high-level distribution networks expansion planning in normal and contingency operation considering reliability. *Electric Power Systems Research* 2021;190:106684.
- [15] Wang, Z., Shen, X., Sun, H., Wu, Q.. A practical urban distribution network planning method with geographic information system. *IEEE Transactions on Power Systems* 2024;.
- [16] Li, Z., Wu, W., Zhang, B., Tai, X.. An milp model for urban distribution network planning considering street layout and block loads. In: 2019 IEEE Power & Energy Society General Meeting (PESGM). IEEE; 2019, p. 1–5.
- [17] Li, S., Zhang, Y., Ling, Z., Zhang, X.. Substation secondary cable path optimization design based on 3d simulation and improved dijkstra algorithm. In: *Journal of Physics: Conference Series*; vol. 2136. IOP Publishing; 2021, p. 012009.
- [18] Youssef, K.H.. Optimal routing and design of radial medium voltage power distribution networks considering cables short circuit withstand-capacity. *IEEE Transactions on Power Delivery* 2022;37(4):2429–2439.
- [19] Skok, M., Skrlec, D., Krajcar, S.. Genetic algorithm and gis enhanced long term planning of large link structured distribution systems. In: *LESCOPE'02. 2002 Large Engineering Systems Conference on Power Engineering. Conference Proceedings*. IEEE; 2002, p. 55–60.
- [20] Göttlicher, M., Wolf, M.. A genetic algorithm for finding microgrid cable layouts. In: *Proceedings of the Thirteenth ACM International Conference on Future Energy Systems*. 2022, p. 1–16.
- [21] Liu, R., Li, J., Chen, Q.. A route optimization method for urban power pipeline network layout. In: *2016 5th International Conference on Computer Science and Network Technology (ICCSNT)*. IEEE; 2016, p. 381–385.
- [22] Zhao, Z., Gao, G., Gan, W., Zhang, J., Wang, Z., Wang, H., et al. Multi-objective optimization for submarine optical cable route planning based on cross reinforcement learning. *Journal of Optical Communications and Networking* 2024;16(10):1018–1033.
- [23] Luo, J., Xu, C., Geng, X., Feng, G., Fang, K., Tan, L., et al. Multistage cable routing through hierarchical imitation learning. *IEEE Transactions on Robotics* 2024;40:1476–1491.
- [24] Wang, X., Kang, Q., Zhou, M., Deng, Q., Fan, Z., Liu, H.. Knowledge classification-assisted evolutionary multitasking for two-task multiobjective optimization problems. *IEEE/CAA Journal of Automatica Sinica* 2025;12(6):1176–1193.
- [25] Liu, F., Zhang, Q., Zhu, Q., Tong, X., Yuan, M.. Machine learning assisted multiobjective evolutionary algorithm for routing and packing. *IEEE Transactions on Evolutionary Computation* 2024;.
- [26] Liu, W., Wang, R., Zhang, T., Li, K., Li, W., Ishibuchi, H., et al. Hybridization of evolutionary algorithm and deep reinforcement learning for multiobjective orienteering optimization. *IEEE Transactions on Evolutionary Computation* 2023;27(5):1260–1274.
- [27] Vidal, T.. Hybrid genetic search for the cvrp: Open-source implementation and swap* neighborhood. *Computers & Operations Research* 2022;140:105643.
- [28] Hart, P.E., Nilsson, N.J., Raphael, B.. A formal basis for the heuristic determination of minimum cost paths. *IEEE transactions on Systems Science and Cybernetics* 1968;4(2):100–107.
- [29] Qiu, A., Yang, Z.. Variable-depth large neighborhood search algorithm for cable routing in distributed photovoltaic systems. *Automation in Construction* 2024;168:105839.
- [30] Monteiro, C., Ramírez-Rosado, I.J., Miranda, V., Zorzano-Santamaría, P.J., García-Garrido, E., Fernández-Jiménez, L.A.. Gis spatial analysis applied to electric line routing optimization. *IEEE transactions on Power Delivery* 2005;20(2):934–942.
- [31] Larsson, J.. Optimizing power cable routing using ai. Master's thesis; Chalmers University of Technology; Gothenburg, Sweden; 2025.
- [32] Trageser, M., Pape, M., Frings, K., Erlinghagen, P., Kurth, M., Vertegwall, C.M., et al. Automated routing of feeders in electrical distribution grids. *Electric Power Systems Research* 2022;211:108217.
- [33] Pavón, W., Inga, E., Simani, S.. Optimal routing an ungrounded electrical distribution system based on heuristic method with micro grids integration. *Sustainability* 2019;11(6):1607.
- [34] Valenzuela, A., Inga, E., Simani, S.. Planning of a resilient underground distribution network using georeferenced data. *Energies* 2019;12(4):644.
- [35] Wang, Z., Lin, D., Zeng, G., Yu, T.. A practical large-scale distribution network planning model based on elite ant-q. *IEEE Access* 2020;8:58912–58922.
- [36] Duvnjak Zarkovic, S., Shayesteh, E., Hilber, P.. Integrated reliability centered distribution system planning—cable routing and switch placement. *Energy Reports* 2021;7:3099–3115.
- [37] Bayliss, C., Hardy, B.. *Transmission and distribution electrical engineering*. Elsevier; 2012.
- [38] Gu, D., Dai, H., Zeng, J.. Full-cable medium voltage distribution network planning based on incremental shortest path method. *Electric*

Power Automation Equipment 2019;39(5):30–44.

[39] Wouda, N.A., Lan, L., Kool, W.. PyVRP: a high-performance VRP solver package. *INFORMS Journal on Computing* 2024;36(4):943–955.

[40] Graves, A.. Long short-term memory. *Supervised sequence labelling with recurrent neural networks* 2012;:37–45.

[41] Vaswani, A., Shazeer, N., Parmar, N., Uszkoreit, J., Jones, L., Gomez, A.N., et al. Attention is all you need. *Advances in neural information processing systems* 2017;30.